JOURNAL OF GUIDANCE, CONTROL, AND DYNAMICS
Vol. 30, No. 4, July–August 2007

Engineering Notes

ENGINEERING NOTES are short manuscripts describing new developments or important results of a preliminary nature. These Notes should not exceed 2500 words (where a figure or table counts as 200 words). Following informal review by the Editors, they may be published within a few months of the date of receipt. Style requirements are the same as for regular contributions (see inside back cover).

Active Control Schemes to Satisfy Separation Distance Constraints

Pedro A. Capó-Lugo* and Peter M. Bainum†
Howard University, Washington, DC 20059

DOI: 10.2514/1.24371

I. Introduction

THE proposed NASA benchmark tetrahedron constellation is a complex formation to be maintained at every apogee point. In previous papers, the authors developed a strategy and determined the initial conditions to maintain the tetrahedron formation [1,2]. With this strategy, the constellation maintains the separation distance constraints for a limited number of orbits, depending on the specific size of the NASA benchmark problem [3]. After a pair of satellites violates the separation distance constraints [1,2], a control strategy is needed to maintain the separation distance conditions [3]. The NASA benchmark problem [3] establishes that the nominal separation distance between any pair of satellites within the constellation is 10 km at the apogee point, and, at any other point in the orbit, the separation distance cannot be less than 1 km.

To explain the dynamics of a pair of satellites in an elliptical orbit, the linearized Tschauner–Hempel (TH) equations are used. In the TH equations, the coefficient term that varies with the true anomaly angle will affect the control scheme that is used to maintain the separation distance between a pair of satellites. The control strategy is based on the linear quadratic regulator (LQR) which was used by Bainum, Strong, and Tan (BST) [4–6]. These authors used the LQR control scheme to maintain the separation between a pair of satellites in an along-track formation (string of pearls), and the varying coefficient was adapted in a piecewise manner. Instead, Carter–Humi (CH) [7,8] used a different approach in which the cost function is defined in terms of the true anomaly angle, and this control scheme will be adapted here to the LQR strategy. These two control schemes will be compared to determine the best response from the BST and CH control approaches. After the constellation is corrected, the Satellite Tool Kit (STK) [9] software is used to propagate the constellation motion and determine when the constellation will again violate the separation distance constraints. Hence, the main objective of this engineering note is to compare and apply these two techniques for the first time to the NASA Benchmark Tetrahedron Constellation to correct the violation of the separation distance constraints [3].

Presented at the AAS/AIAA Space Flight Mechanics Conference, Tampa, FL, 22–26 January 2006; received 31 March 2006; revision received 22 January 2007; accepted for publication 6 February 2007.

*Graduate Student, Department of Mechanical Engineering; pcapo@howard.edu. Member AIAA.

†Corresponding Author, Distinguished Professor of Aerospace Engineering, Emeritus, Department of Mechanical Engineering; pbainum@fac.howard.edu. Fellow AIAA.

II. Definition of the Specific Sizes (or Phases)

The benchmark problem has four phases with a mission period of two years, but this research is only concerned with the three phases that contain the restrictions to maintain the separation distance constraints. These three phases are detailed in Table 1 [1,2] in terms of the orbital elements. The fourth phase for the NASA benchmark problem is a lunar swing-by, which is not considered here.

In Table 1, ER means Earth radius. The inclination angle in the third phase is not specified in the benchmark problem [3] because the constellation must be in a near-polar orbit, and this orbital inclination angle is chosen to be 85 deg. Through this paper, phase 2 of the benchmark problem will be analyzed with the active control schemes.

III. Linearized Tschauner–Hempel Equations

The derivation of the linearized TH equations follows the same procedure as CH [8], in which they derived a set of equations to describe the rendezvous motion between a pair of satellites in an elliptical orbit for a general Keplerian orbit. For this application, the separation distance between a pair of satellites within the constellation is needed to be maintained at the apogee point to satisfy the separation distance constraints of the NASA benchmark problem [3]. From [8], Carter–Humi developed a set of equations, which explains the movement of a maneuvering spacecraft relative to the reference satellite in an elliptical orbit as

$$y_1'' = 2y_2' + a_1 \qquad y_2'' = 3\kappa y_2 - 2y_1' + a_2 \qquad y_3'' = -y_3 + a_3 \tag{1a}$$

where

$$\kappa = \frac{\mu r}{h^2} = \frac{1}{1 + e\cos\theta} \tag{1b}$$

$$a_j = \frac{T_j}{m}\left(\frac{h^6}{\mu^4}\right)(1 + e\cos\theta)^{-3}; \qquad j = 1, 2, 3 \tag{1c}$$

$$()' = \frac{\mathrm{d}()}{\mathrm{d}\theta} \qquad ()'' = \frac{\mathrm{d}^2()}{\mathrm{d}^2\theta} \tag{1d}$$

$$y_j = (1 + e\cos\theta)x_j \qquad y_j' = (1 + e\cos\theta)x_j' - (e\sin\theta)x_j$$
$$y_j'' = (1 + e\cos\theta)x_j'' - (2e\sin\theta)x_j' - (e\cos\theta)x_j \tag{2}$$

κ is determined from the well-known equation of a Keplerian orbit (or equation of a conic section) where $\mu = GM_E$, r is the radial position of the satellite at any point in the orbit, h is the angular momentum, and θ is the true anomaly angle. x_1 is positive against the motion of the spacecraft, x_2 is positive along the radial direction, and x_3 is positive when the right-handed system is completed. Equation (2) is the mathematical transformation used to change from the x_j system to the y_j system. The x_j system contains the actual separation distance between the maneuvering and the reference (or target) spacecraft, and the y_j system has the same specified directions as the x_j system. The maneuvering spacecraft is assumed to have an

Table 1 Dimensions for the three phases

Dimensions	First phase	Second phase	Third phase
Radius of perigee r_p	1.2 ER	1.2 ER	10 ER
Radius of apogee r_a	12 ER	30 ER	40 ER
Semimajor axis a	42,095.7 km	99,498.92 km	159,453.4 km
Eccentricity e	0.818	0.923	0.6
Inclination angle i	18.5 deg	18.5 deg	85.0 deg
Period, days	1	3.6	7

applied thrust vector along the reference coordinate system, and the reference (or target) spacecraft is initially assumed to be acted on by a Newtonian gravitational force directed toward the center of the Earth. Equations (1a) are called the linearized rendezvous TH equations for the motion of a pair of satellites in an elliptical orbit. A control function [10] $u(\theta)$ can be used to represent the change in thrust $T(\theta)$ and mass $m(\theta)$ with respect to the true anomaly angle as

$$\frac{T_m}{m_0}u_j(\theta) = \frac{T_j(\theta)}{m(\theta)} \tag{3}$$

where T_m and m_0, respectively, are the maximum thrust and initial mass of the maneuvering satellite. If

$$\nu = \frac{h^6}{\mu^4}\frac{T_m}{m_0} \tag{4a}$$

the new state variables [10] can be written as,

$$\xi = \frac{y_1}{\nu} \qquad \varsigma = \frac{y_2}{\nu} \qquad \eta = \frac{y_3}{\nu} \tag{4b}$$

Using Eqs. (3) and (4), the linearized equations for the motion of the maneuvering satellite [Eq. (1a)], in state-based format, can be defined in the following form [10]:

$$\begin{bmatrix} \xi' \\ \varsigma' \\ \eta' \\ \xi'' \\ \varsigma'' \\ \eta'' \end{bmatrix} = \begin{bmatrix} 0 & 0 & 0 & 1 & 0 & 0 \\ 0 & 0 & 0 & 0 & 1 & 0 \\ 0 & 0 & 0 & 0 & 0 & 1 \\ 0 & 0 & 0 & 0 & 2 & 0 \\ 0 & 3\kappa & 0 & -2 & 0 & 0 \\ 0 & 0 & -1 & 0 & 0 & 0 \end{bmatrix} \begin{bmatrix} \xi \\ \varsigma \\ \eta \\ \xi' \\ \varsigma' \\ \eta' \end{bmatrix} + \begin{bmatrix} 0 & 0 & 0 \\ 0 & 0 & 0 \\ 0 & 0 & 0 \\ \kappa^3 & 0 & 0 \\ 0 & \kappa^3 & 0 \\ 0 & 0 & \kappa^3 \end{bmatrix} \begin{bmatrix} u_1 \\ u_2 \\ u_3 \end{bmatrix} \tag{5}$$

A. Bainum, Strong, and Tan Approach

For BST [4–6], $\kappa = \mu r/h^2$, and the nonlinear coefficient term is adapted in a piecewise manner. The active control scheme used by these authors is the LQR. To determine this active control law, the following quadratic cost function is used:

$$J = \frac{1}{2}\int_{\theta_0}^{\theta_f} (\{[x(\theta) - x_D]^T Q[x(\theta) - x_D]\} + \{[u(\theta)]^T R[u(\theta)]\})\,\mathrm{d}\theta \tag{6}$$

where $x(\theta)$ is the state vector, and x_D is the desired state vector. $u(\theta)$ is the control signal that will be used to maintain the separation distance constraints. Q and R are weight functioning matrices in which Q is a $n \times n$ positive semidefinite matrix, and R is a $m \times m$ positive definite matrix. This cost function is used to minimize the difference in the errors between the state vectors and the desired state vectors.

B. Carter–Humi Approach

CH [7,8] used the same linearized TH equations, but $\kappa = 1/(1 + e\cos\theta)$. For CH, certain terms in the coefficient matrices are varying with the true anomaly angle θ. CH [7] used Pontryagin minimum principles to obtain an admissible control such that the control scheme is used to effect a rendezvous in an optimal way between a pair of satellites. For the LQR scheme here, the cost function is defined in terms of the varying term in the state matrix [Eq. (5)] and the cost function defined by CH:

$$J = \frac{1}{2}\int_{\theta_0}^{\theta_f} \left\{ \left[\frac{[x(\theta) - x_D]^T Q[x(\theta) - x_D]}{1 + e\cos\theta}\right] + \left[\frac{[u(\theta)]^T R[u(\theta)]}{(1 + e\cos\theta)^2}\right] \right\} \mathrm{d}\theta \tag{7}$$

IV. Development of the Linear Quadratic Regulator Optimal Control

The LQR optimal control will be implemented with the use of the cost function defined by Eq. (6), and the same LQR strategy can be implemented for the cost function in Eq. (7). The solution of the LQR problem leads to an optimal feedback system with the property that the components of the state vector $x(\theta)$ are kept near the desired state vector x_D without excessive expenditure of control energy [10]. The existence of the optimal control is obtained from the solution of the Hamilton–Jacobi equation, which is defined everywhere to obtain a minimum-time problem. Considering the angle-varying system similar to Eq. (5) but also containing the effects of perturbations due to the Earth's oblateness, the state vector system can be written as

$$x'(\theta) = A(\theta)x(\theta) + B(\theta)u(\theta) + \psi(\theta) \tag{8}$$

In Eq. (8), $\psi(\theta)$ is a $n \times 1$ disturbance column matrix. The A and B matrices, respectively, have a dimension of $n \times n$ and $n \times m$. The Hamiltonian H for the state-based system (8) and the cost function (6) can be defined as

$$H = \frac{1}{2}\|x(\theta) - x_D\|^2 Q + \frac{1}{2}\|u(\theta)\|^2 R + \overline{[A(\theta)x(\theta)]} \cdot \overline{p(\theta)} + \overline{[B(\theta)u(\theta)]} \cdot \overline{p(\theta)} + \overline{\psi(\theta)} \cdot \overline{p(\theta)} \tag{9}$$

where superbarred quantities indicate vectors and dot $(\cdot)$ refers to vector dot product. The minimum principles are used to obtain the necessary conditions for the optimal control, and, when the control scheme is defined continuously in the true anomaly angle, the solution of the LQR problem is expressed as [10,11]

$$-A^T(\theta)k(\theta) - k(\theta)A(\theta) + k(\theta)S(\theta)k(\theta) - Q = 0 \tag{10a}$$

$$m(\theta) = [A^T(\theta) + k(\theta)S(\theta)]^{-1}[Qx_D - k(\theta)\psi(\theta)] \tag{10b}$$

$$x'(\theta) = A(\theta)x(\theta) - S(\theta)k(\theta)x(\theta) - S(\theta)m(\theta) + \psi(\theta) \tag{10c}$$

$$u(\theta) = -S(\theta)[k(\theta)x(\theta) + m(\theta)] \tag{10d}$$

$$S(\theta) = B(\theta)R^{-1}B^T(\theta) \tag{10e}$$

Equations (10a) and (10b), respectively, are the Ricatti equation and the adjoint Ricatti equation, and these equations are solved continuously in the true anomaly angle as shown in [10]. $k(\theta)$ and $m(\theta)$ have an $n \times n$ and $n \times 1$ dimension, respectively. The state vector is solved using a numerical integration scheme such as the Runge–Kutta method [12] because this integration process runs forward in time, and the control vector [Eq. (10d)] is determined with the solutions of Eqs. (10a–10c). Equations (10) are used to solve the LQR control scheme for the BST approach. By solving the LQR approach with Eq. (7) (CH approach) and (8), Eqs. (10) will be

obtained, but the Q and R can be rewritten, respectively, as $\tilde{Q} = Q\kappa$and $\tilde{R} = R\kappa^2$ [where $\kappa = (1 + e\cos\theta)^{-1}$] because of the definition of the cost function in Eq. (7).

V. Results

The simulations of the BST and CH active control schemes are tested with the conditions shown in Table 1 for phase 2. The initial conditions are calculated from the difference between the nominal and the relative separation distance between a pair of satellites. This difference is the error in the separation distance that must be corrected. The desired state vector [Eqs. (6) and (7)], x_D, is set equal to zero. The relative distance between a pair of satellites is taken from the simulations performed by the STK [9]. The disturbance matrix in Eq. (8) will contain the J2 perturbation as defined in [13] according to

$$\psi(\theta) = \begin{bmatrix} 0 \\ 0 \\ 0 \\ -\frac{3}{2}J_2\frac{\mu}{r^2}\left(\frac{R_e}{r}\right)^2(1 - 3\sin^2 i\sin^2\theta) \\ -3J_2\frac{\mu}{r^2}\left(\frac{R_e}{r}\right)^2(\sin^2 i\sin\theta\cos\theta) \\ -3J_2\frac{\mu}{r^2}\left(\frac{R_e}{r}\right)^2(\sin i\cos i\sin\theta) \end{bmatrix}$$

where J_2 is approximated to 1.08263×10^{-3}, R_e is the radius of the earth, and i is the inclination angle.

The initial conditions are defined as

$$x(\theta_0)^T = [-1.18 \quad 0.302 \quad 0.012 \quad 2.15\times10^{-4} \quad -1.4\times10^{-5} \quad -9\times10^{-06}]^T$$

The numerical values are taken from the apogee point (θ_0) where the separation distance constraints are first violated. Bainum et al. [6] and Strong [11] explain how the BST control scheme defines the varying coefficient term in a piecewise manner.

Q is a 6×6 diagonal matrix with a value of 20, and R is a 3×3 diagonal matrix with a value of 10 for all nonzero elements. Figure 1 shows the responses for the position, the velocity, and the optimal control for the BST and CH control schemes. In this case, the BST active control scheme shows a different response in comparison to the CH active control scheme. The BST control scheme shows a high peak in the position, velocity, and optimal control; however, the CH active control scheme comes into steady state in approximately 6 h. This difference between the responses is due to the changes in the orbital elements, in particular the much larger eccentricity for phase 2. In Eq. (7), the CH active control scheme uses the eccentricity and the true anomaly angle to vary the weights in the Q and R matrices. In the BST active control scheme, the Q and R matrices are maintained constant while the varying term in the state matrix is adapted in a piecewise manner. The results here for phase 2 show that the piecewise adapted BST active control scheme may be limited to smaller values of the eccentricity. This tendency is indicated by additional simulations not shown here but available in [14].

To address this limitation on the magnitude of the eccentricity for phase 2, a different approach can be taken. This approach consists of increasing the weights in the Q and R matrices and/or using different or split weights for the diagonal terms. The positions (ξ, ς, η) are weighted more than the velocities $(\xi', \varsigma', \eta')$ as follows: $Q = \text{diag}[20 \quad 20 \quad 20 \quad 1 \quad 1 \quad 1]$ and $R = \text{diag}[20 \quad 20 \quad 20]$. In Eq. (5), the positions of the satellite are multiplied by the varying coefficient terms, and the velocities are multiplied by constants. It can be seen that, by weighting more the positions, the LQR control scheme will compensate more the varying coefficient terms than the velocities in Eq. (5). Figure 2 shows the responses for the correction in the positions and velocities between a pair of satellites within the constellation. For these initial conditions, the system of linear equations gives a steady-state solution in which the CH active control scheme requires a lower thrust level than for the BST. In both active control schemes, the system comes into steady state in less than 4 h. The BST active control scheme comes to steady state faster than in the CH active control scheme because the varying coefficient term is adapted piecewisely. In Fig. 1, the system does not achieve a steady response because the varying coefficient term has the same weight as the velocities ($Q = \text{diag}[20 \quad 20 \quad 20 \quad 20 \quad 20 \quad 20]$). Once the Q matrix is changed to place more weight on the positions, the system results in a steady-state solution for both active control schemes.

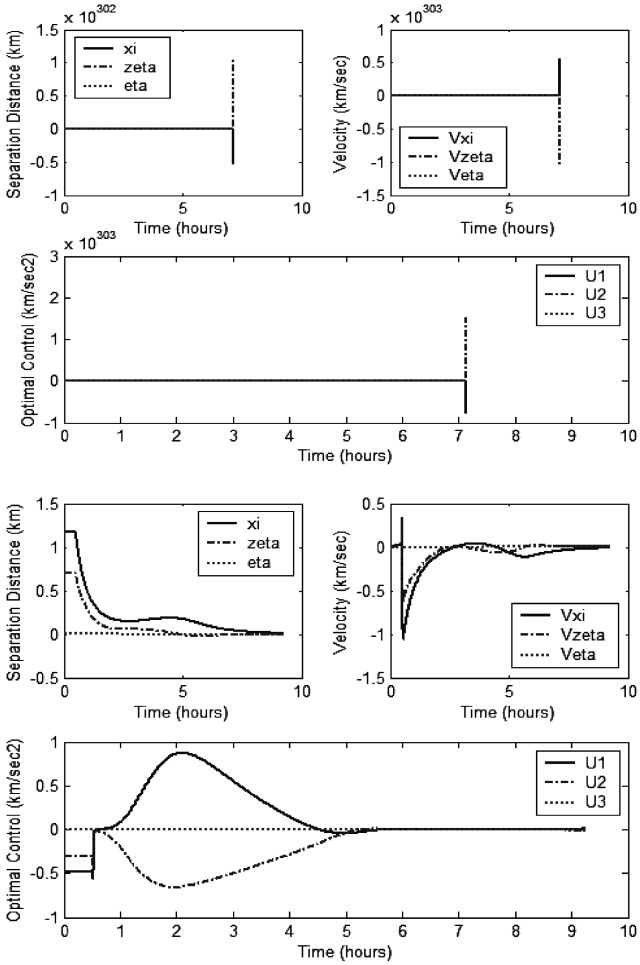

Fig. 1 Separation distance correction using BST (top) and CH (bottom) active control scheme, $Q = \text{diag}[20 \quad 20 \quad 20 \quad 20 \quad 20 \quad 20]$ and $R = \text{diag}[10 \quad 10 \quad 10]$ for phase 2.

VI. Examination of the Drifts After the First Correction

The Satellite Tool Kit software [9] is used to propagate the constellation after the active control scheme has corrected the drift between the pair of satellites that violate the NASA benchmark tetrahedron conditions first [1,2,14]. The STK is used to propagate the motion of this pair of satellites at the apogee point after the correction is made. For phase 2, Table 2 [1,2] shows the initial conditions at the initial apogee point for this pair of satellites. After

Table 2 Initial coordinates and velocities for phase 2

Axis	Reference satellite	Maneuvering satellite
X, km	−8.66025403	0
Y, km	−179, 772.5402	−179, 767.8426
Z, km	−65, 531.6439	−65, 529.9315
V_x, km/s	0.400303769	0.400439734
V_y, km/s	0	0
V_z, km/s	0	0

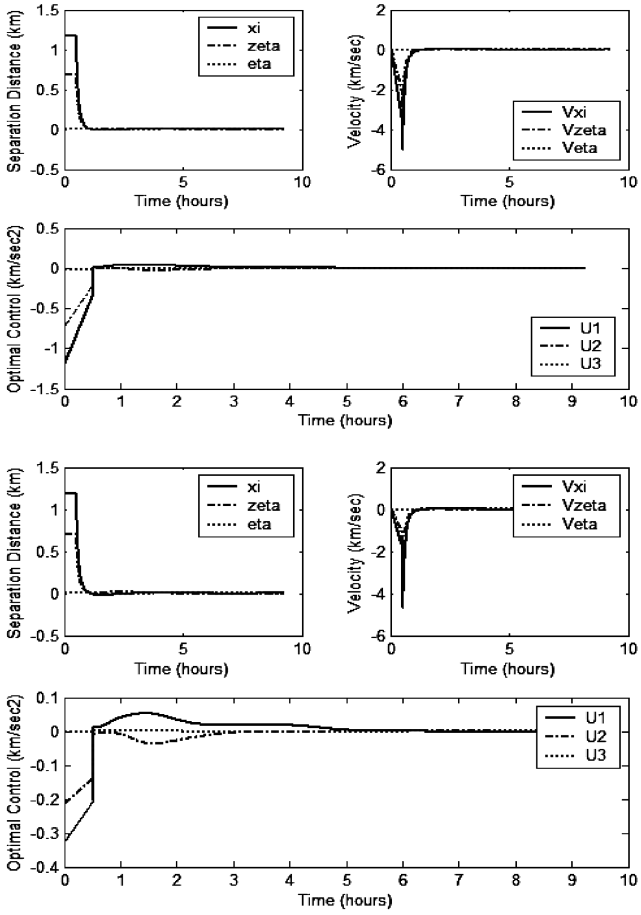

Fig. 2 Separation distance correction using BST (top) and CH (bottom) active control scheme, $Q = \mathrm{diag}[\,20 \quad 20 \quad 20 \quad 1 \quad 1 \quad 1\,]$ and $R = \mathrm{diag}[\,20 \quad 20 \quad 20\,]$ for phase 2.

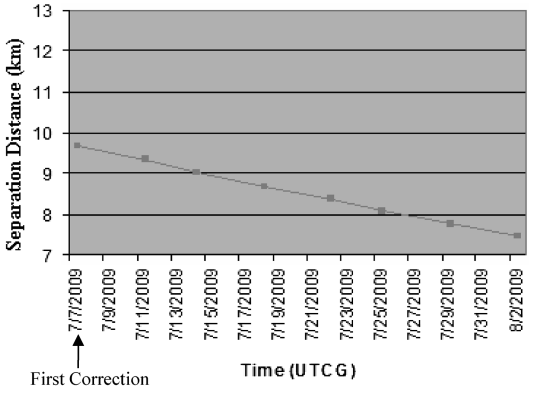

Fig. 3 Separation distance of the satellites in the in-plane motion with J2 perturbation only for phase 2.

using different weights and initial conditions [14], the solution of the LQR for both control approaches provided an approximate very small steady-state error for the correction of the positions and velocities equal to 1×10^{-6} for the positions (km) and velocities (km/s). This steady-state error is added to the initial conditions shown in Table 2 to determine the amount of time before the separation distance constraints are again violated. Figure 3 shows the separation distance for this pair of satellites when only the J2 perturbation is present. The constellation satisfies the separation distance constraints for three complete orbits.

VII. Conclusions

This engineering note contributes, for the first time to our knowledge, to the application of two linear quadratic regulator control schemes to the NASA benchmark tetrahedron constellation and compares both techniques. Through this note, it can be seen that the Carter–Humi active control scheme provides a better response to the correction of the drifts and control consumption than the Bainum, Strong, and Tan active control approach because the eccentricity and the true anomaly angle are part of the formulation; also, the Carter–Humi active control scheme can be applied for every eccentricity and sets of weighting matrices. In addition, for the first time, an examination of the drifts in separation distances can be used to predict when the separation distance constraints will be violated again.

Acknowledgment

Research supported by NSF Alliances for Graduate Education and Professoriate (AGEP) Program.

References

[1] Capó-Lugo, P. A., and Bainum, P. M., "Strategy for Satisfying Distance Constraints for the NASA Benchmark Tetrahedron Constellation," AAS Paper 05-153, Jan. 2005.

[2] Capó-Lugo, P. A., and Bainum, P. M., "Implementation of the Strategy for Satisfying Distance Constraints for the NASA Benchmark Tetrahedron Constellations," AAS Paper 05-344, Aug. 2005.

[3] Carpenter, R. J., Leitner, J. A., Burns, R. D., and Folta, D. C., "Benchmark Problems for Spacecraft Formation Flying Missions," AIAA Paper 2003-5364, Aug. 2003.

[4] Tan, Z., Bainum, P. M., and Strong, A., "A Strategy for Maintaining Distance Between Satellites in an Orbiting Constellation," AAS Paper 99-125, Feb. 1999.

[5] Tan, Z., Bainum, P. M., and Strong, A., "The Implementation of Maintaining Constant Distance Between Satellites in Coplanar Elliptic Orbits," *Journal of the Astronautical Sciences*, Vol. 50, No. 1, Jan.–March 2002, pp. 53–69.

[6] Bainum, P. M., Tan, Z., and Duan, X., "Review of Station Keeping for Elliptically Orbiting Constellations in Along-Track Configuration," *International Journal of Solids and Structures* (PACAM VIII Special Issue), Vol. 42, Nos. 21–22, Oct. 2005, pp. 5683–5691.

[7] Carter, T., and Humi, M., "Fuel-Optimal Rendezvous Near a Point in General Keplerian Orbit," *Journal of Guidance, Control, and Dynamics*, Vol. 10, No. 6, Nov.–Dec. 1987, pp. 567–573.

[8] Carter, T., "New Form for the Optimal Rendezvous Equations Near a Keplerian Orbit," *Journal of Guidance, Control, and Dynamics*, Vol. 13, No. 1, Jan.–Feb. 1990, pp. 183–186.

[9] STK, Satellite Tool Kit Software, Ver. 5.0, Analytical Graphics, Inc., Malvern, PA, 2003.

[10] Athans, M., and Falb, P. L., *Optimal Control, An Introduction to the Theory and its Applications*, McGraw–Hill, New York, 1966.

[11] Strong, A., "On the Deployment and Station Keeping Dynamics of N-Body Orbiting Satellite Constellations," Ph.D. Dissertation, Howard Univ., Washington, DC, 2000.

[12] Strang, G., *Introduction to Applied Mathematics*, Wellesley–Cambridge Press, Cambridge, MA, 1986.

[13] Mishne, D., "Controlling the Out-of-Plane Motion of a Follower Satellite in a Periodical Relative Trajectory, Using Angular Rate Information," AIAA Paper 2004-5215, Aug. 2004.

[14] Capó-Lugo, P. A., "Strategies and Control Schemes to Satisfy the Separation Distance Constraints for the NASA Benchmark Tetrahedron Constellation," M.S. Thesis, Howard Univ., Washington, DC, Dec. 2005.